

Stiffness Matrix for Haunched Members With Including Effect of Transverse Shear Deformations

Abbas Abdel-Majid Allawi*

Received on: 22/9/2004

Accepted on: 13/3/2005

Abstract

This study includes the derivation of the stiffness matrix for a haunched member using the simple bending theory. The derived stiffness matrix covers most possible geometric shapes for haunched members under different loading cases and combinations with including transverse shear deformations effect. The importance of the transverse shear deformation in haunched members with high depth to span ratios is shown using numerical example. The accuracy of the proposed analysis technique is verified by comparing the results of the numerical example with those obtained from the general analysis program SAP90 using a large number of subelements.

مصفوفة الجساءة للاعضاء ذات النهايات
المثخنة متضمنة ادخال تأثير تشوهات القص العرضي

الخلاصة

هذه الدراسة تتضمن اشتقاق مصفوفة الجساءة للاعضاء الانشائية المثخنة عند النهايات استنادا على نظرية الانحناء البسيطة. مصفوفة الجساءة التي تم اشتقاقها تغطي معظم الاشكال الهندسية لهذه العتبات تحت تأثير مختلف حالات التحميل والتداخل في الاحمال مع ادخال تأثير تشوهات القص العرضي. ان اهمية تأثير تشوهات القص العرضي لهذه الاعضاء ذات نسبة عمق الى فضاء عالية قد جرى توضيحها في مثال عددي. وجرى اختبار دقة طريقة التحليل المقترحة بمقارنة النتائج للمثال العددي مع تلك المستحصلة من نتائج التحليل باستخدام برنامج التحليل SAP90 باستخدام عدد كبير من العناصر.

Introduction

Haunched members can be used to shape the members in accordance with the distribution of the internal stress. By using these types of members, one can achieve the required strength with the minimum weight and material and also may satisfy architectural or functional requirements. In industrial buildings, bridges, and high rise buildings, non-prismatic members with variable depth or width are usually used.

Different approaches have been developed for the analysis of non-

prismatic members (Including haunched members). Reynolds and Steedman (1988) published tables and graphs for analysis purposes. Similar calculations are also given in other textbooks, for example by Timoshenko and Young (1965), Vanderbilt (1978) and Funk and Wang (1988) calculated the stiffness matrix and fixed end forces by dividing the non-prismatic member into subelements.

A refined analysis can be performed by deriving the stiffness matrix and fixed end forces by

considering the exact variations of the geometry. Al-Gahtani (1996) derived the stiffness matrix by using differential equations and determined fixed end forces for distributed and concentrated member loads. Timoshenko and Young (1965) concluded that if the variation of the cross section of a non-prismatic member is not too rapid, it can be analyzed with sufficient accuracy by using the prismatic beam equations. Al-Mezani and Balkaya (1991) demonstrated the problems due to discontinuity of member axis and arching effect in analyzing non-prismatic members.

The use of tables and graphs is limited to certain cross sections and span loads and is also difficult if several loading may be considered. In the case of computer applications, dividing the members into subelements increases the number of equations and requires a larger amount of input data. Therefore, most of latest studies have focused on a stiffness formulation of non-prismatic members, which considered the exact variation of the geometry. The effect of shear deformations on fixed end forces has not been considered so far for non-prismatic members.

The purpose of this study is to develop an exact solution using the simple bending theory for non-prismatic members with a wide range of span load variations and finite element formulation.

Stiffness Matrix:

The haunched members with a rectangular cross section and length L as shown in Fig. 1 is assumed to be made of homogeneous, isotropic and linearly elastic materials. Stiffness Matrix:

The haunched members with a rectangular cross section and length L as shown in Fig. 1 is assumed to be made of homogeneous, isotropic and linearly elastic materials. Member end displacements, \mathbf{U} , forces \mathbf{F} , and fixed end forces \mathbf{P} are shown in Fig. 2.

The displacement method yields the following member equilibrium equation:

$$\mathbf{F} = \mathbf{K} \cdot \mathbf{U} + \mathbf{P} \quad (1)$$

where \mathbf{K} is the general stiffness matrix of a non-prismatic member. Based on the conjugate beam method (Norriss et. al. 1982), \mathbf{K} can be suggested to be as follows:

$$\begin{bmatrix} n_{ii} \frac{EA_0}{L} & 0 & 0 & -n_{ii} \frac{EA_0}{L} & 0 & 0 \\ 0 & (m_{ii} + m_{jj} + 2m_{ij}) \frac{EI_0}{L^3} b & (m_{ii} + m_{ij}) \frac{EI_0}{L^2} b & 0 & -(m_{ii} + m_{jj} + 2m_{ij}) \frac{EI_0}{L^3} b & (m_{jj} + m_{ij}) \frac{EI_0}{L^2} b \\ 0 & (m_{ii} + m_{ij}) \frac{EI_0}{L^2} b & m_{ii} \frac{EI_0}{L} \Gamma_1 & 0 & -(m_{ii} + m_{ij}) \frac{EI_0}{L^2} b & m_{ij} \frac{EI_0}{L} \Gamma_2 \\ -n_{ii} \frac{EA_0}{L} & 0 & 0 & n_{ii} \frac{EA_0}{L} & 0 & 0 \\ 0 & -(m_{ii} + m_{jj} + 2m_{ij}) \frac{EI_0}{L^3} b & -(m_{ii} + m_{ij}) \frac{EI_0}{L^2} b & 0 & (m_{ii} + m_{jj} + 2m_{ij}) \frac{EI_0}{L^3} b & -(m_{jj} + m_{ij}) \frac{EI_0}{L^2} b \\ 0 & (m_{jj} + m_{ij}) \frac{EI_0}{L^2} b & m_{ij} \frac{EI_0}{L} \Gamma_2 & 0 & -(m_{jj} + m_{ij}) \frac{EI_0}{L^2} b & m_{jj} \frac{EI_0}{L} \Gamma_3 \end{bmatrix}$$

where A_0 and I_0 are the area and moment of inertia for the prismatic part of haunched member respectively and E is the modulus of elasticity.

The effect of the variation of the area is expressed by the coefficients n_{ii} and the variation of the moment of inertia by the coefficients m_{ii} , m_{ij} , and m_{jj} . When the member is prismatic, $n_{ii}=1$, $m_{ii}=m_{ij}=m_{jj}=4$ and $m_{ij}=2$. The factors β , Γ_1 , Γ_2 and Γ_3 account for the shear effect. In the case of Bernoulli-Euler theory, $\beta = \Gamma_1 = \Gamma_2 = \Gamma_3 = 1$ (no transverse shear effect). However, especially for members with high depth to span ratios, shear deformations should be considered to increase the accuracy.

The coefficients m_{ii} , m_{ij} and m_{jj} are determined by using the conjugate beam method and n_{ii} is derived from the force-deformation. Fig. 3a shows the corresponding forces and couples when $\mathbf{P} = \mathbf{0}$, $U_3 = 1$, and all other displacements are zero in eq. (1). $M(x)/EI(x)$ is applied as load to the conjugate beam as shown in Fig. 3d.

From the equilibrium at the i and j ends, the following equations are obtained:

$$-AL - m_{ii} \frac{EI_0}{L^2} \int_0^L \frac{(L-x)^2}{EI(x)} dx + m_{ij} \frac{EI_0}{L^2} \int_0^L \frac{x(L-x)}{EI(x)} dx = 0 \quad (3)$$

$$BL + m_{ii} \frac{EI_0}{L^2} \int_0^L \frac{x(L-x)}{EI(x)} dx - m_{ij} \frac{EI_0}{L^2} \int_0^L \frac{x^2}{EI(x)} dx = 0 \quad (4)$$

Denoting the integral as:

$$I_1 = \int_0^L \frac{x^2}{EI(x)} dx, \quad I_2 = \int_0^L \frac{1}{EI(x)} dx, \quad I_3 = \int_0^L \frac{x}{EI(x)} dx \quad (5)$$

then equations (3) and (4) can be rewritten in the form:

$$\begin{bmatrix} A \\ B \end{bmatrix} = \frac{I_0}{L^3} \begin{bmatrix} -L^2 I_2 + 2LI_3 - I_1 & LI_3 - I_1 \\ -LI_3 + I_1 & I_1 \end{bmatrix} \times \begin{bmatrix} m_{ii} \\ m_{ij} \end{bmatrix} \quad (6)$$

where $A = -1$ and $B=0$ in this case.

Imposing a unit displacement $U_6 = 1$, similar equations can be written in terms of m_{ii} and m_{ij} for the case of $A=0$ and $B=1$. Denoting the matrix of the coefficients in eq.(6) by \mathbf{C} then for $U_3 = 1$, and $U_6 = 0$ and for $U_3 = 0$, and $U_6 = 1$, the following systems are obtained:

$$\mathbf{C} \begin{bmatrix} m_{ii} \\ m_{ij} \end{bmatrix} = \begin{bmatrix} -1 \\ 0 \end{bmatrix}, \quad \mathbf{C} \begin{bmatrix} m_{ij} \\ m_{jj} \end{bmatrix} = \begin{bmatrix} 0 \\ 1 \end{bmatrix} \quad (7)$$

This yield

$$m_{ii} = \frac{I_1}{\det C}, \quad m_{ijh} = \frac{LI_3 - I_1}{\det C}, \quad m_{jj} = \frac{-L^2 I_2 + 2LI_3 - I_1}{\det C} \quad (8)$$

$$\text{where } \det C = -\frac{I_0}{L} (I_1 I_2 - I_3^2) \quad (9)$$

when $\mathbf{P}=\mathbf{0}$, and $U_1 = 1$ and all other displacements are zero in eq. (1), an axial force of magnitude $n_{ii} EA_0/L$ is developed. Then the force-deformation relation gives:

$$\Delta L = 1 = n_{ii} \frac{EA_0}{L} \int_0^L \frac{1}{EA(x)} dx \quad (10)$$

Solving eq. (10) for the unknown n_{ii} yields:

$$n_{ii} = \frac{L}{A_0} \frac{1}{\int_0^L (1/A(x)) dx} = \frac{L}{A_0 I_4} \quad (11)$$

where

$$I_4 = \int_0^L \frac{1}{A(x)} dx \quad (12)$$

Determination of the factors n_{ii} , m_{ii} and m_{ij} of the basic stiffness coefficients is based on the evaluation of the integrals of eqs. (5) and (12). The integrals I_1 , I_2 , I_3 and I_4 for the selected member types can be calculated for different haunch shapes according to the taper factors α_i and α_j at ends (see Appendix (A)). A hunched member is assumed to be consisting of three segments as shown in Fig. 1. The moment of inertia and the area in the regions with length L_i and L_j are variable and in the region with length L_o are constant. The integrals I_1 , I_2 , I_3 and I_4 represent the summation of these three components. Integrals for the constant and linear variations can be performed analytically, while for any curved variation, numerical integration is suggested to be done.

Stiffness Factors for Shear Effect:

Neglecting axial deformations and partitioning the matrices into four 2 x 2 submatrices, the beam stiffness matrices can be represented respectively in the following simplified forms:

$$\bar{k} = \begin{bmatrix} \bar{k}_{11} & \bar{k}_{12} \\ \bar{k}_{21} & \bar{k}_{22} \end{bmatrix}, \quad \bar{k} = \begin{bmatrix} \bar{\bar{k}}_{11} & \bar{\bar{k}}_{12} \\ \bar{\bar{k}}_{21} & \bar{\bar{k}}_{22} \end{bmatrix} \quad (13)$$

The stiffness matrix of the member shown in Fig. 4 corresponding to the coordinates F_2 and F_3 is:

$$\bar{k}_{11} = \begin{bmatrix} \frac{(m_{ii} + m_{jj} + 2m_{ij})EI_0}{L^3} & \frac{(m_{ii} + m_{ij})EI_0}{L^2} \\ \frac{(m_{ii} + m_{ij})EI_0}{L^2} & \frac{m_{ij}EI_0}{L} \end{bmatrix} \quad (14)$$

Using the relation between the transverse shearing deformations and applied shearing forces, shear deflection due to unit transverse load at end i can be expressed as Popov (1968):

$$U_{2_{shear}} = \frac{a}{G} \int_0^L \frac{1}{A(x)} dx = \frac{aI_4}{G} \quad (15)$$

where G is the shear modulus and α is the shape factor of the cross section for shear.

The following notation is used:

$$y = \frac{aI_4}{G} \frac{(m_{ii}m_{jj} - m_{ij}^2)EI_0}{m_{ii}L^3} \quad (16)$$

Shear deformation can be added to the inverse of eq. (14), i.e., the flexibility matrix as:

$$\bar{\bar{k}}_{11}^{-1} = \begin{bmatrix} \frac{m_{ii}L^3(1+y)}{(m_{ii}m_{jj} - m_{ij}^2)EI_0} & -\frac{(m_{ii} + m_{ij})L^2}{(m_{ii}m_{jj} - m_{ij}^2)EI_0} \\ -\frac{(m_{ii} + m_{ij})L^2}{(m_{ii}m_{jj} - m_{ij}^2)EI_0} & \frac{(m_{ii} + m_{jj} + 2m_{ij})L}{(m_{ii}m_{jj} - m_{ij}^2)EI_0} \end{bmatrix} \quad (17)$$

The stiffness matrix \bar{k}_{11} by considering the transverse shear deformation can be obtained by inverting eq. (17). The matrix \bar{k}_{21} can be obtained from the equilibrium conditions of the member. Repeating the outlined procedure for the cantilever, by considering joint i as fixed end and releasing joint j , \bar{k}_{22} and \bar{k}_{12} can be obtained similarly. The multiplication factors β , Γ_1 , Γ_2 and Γ_3 are given as follows:

$$b = \frac{GL^3}{EI_0 I_4 (m_{ii} + m_{jj} + 2m_{ij}) + L^3 G} \quad (18)$$

$$\Gamma_1 = \left\{ \frac{EI_0 I_4 (m_{ii} m_{jj} - m_{ij}^2)}{m_{jj} L^3 G} + 1 \right\} b \quad (19)$$

$$\Gamma_1 = \left\{ \frac{-EI_0 I_4 (m_{ii} m_{jj} - m_{ij}^2)}{m_{jj} L^3 G} + 1 \right\} b \quad (20)$$

$$\Gamma_1 = \left\{ \frac{EI_0 I_4 (m_{ii} m_{jj} - m_{ij}^2)}{m_{jj} L^3 G} + 1 \right\} b \quad (21)$$

Fixed End Forces Due to Axial Forces:

Fixed end forces for the axially loaded non-prismatic member are derived using the flexibility method. Referring to Fig. 5, static equilibrium yields:

$$\mathbf{P}_1 + \mathbf{P}_2 = -\mathbf{Q} \quad (22)$$

Choosing \mathbf{P}_1 as a redundant and loading the primary structure with the actual load \mathbf{Q} , the displacement of point i due to \mathbf{P}_1 is:

$$d_{P_1} = \frac{P_1}{n_{ii} A_0 E / L} = \frac{P_1 I_4}{E} \quad (23)$$

and the displacement of point i due to the actual force \mathbf{Q} is :

$$d_Q = \frac{Q}{\bar{n}_{ii} \bar{A}_0 E / \bar{L}} = \frac{Q I_5}{E} \quad (24)$$

where \bar{A}_0 is the minimum area along the length \bar{L} ,

$$\bar{n}_{ii} = \frac{\bar{L}}{A_0} \frac{1}{\int_0^{\bar{L}} (1/A(x)) dx} \quad (25a) \text{ and}$$

$$I_5 = \int_0^{\bar{L}} (1/A(x)) dx \quad (25b)$$

Using compatibility at point i and the equilibrium condition (eq. (22)), then:

$$p_4 = -\frac{Q I_5}{I_4} \quad (26)$$

and

$$p_4 = Q \left(\frac{I_5}{I_4} - 1 \right) \quad (27)$$

Fixed End Forces Due to Bending and Shear :

The rest of the span loads considered are perpendicular to the member axis, therefore $\mathbf{P}_1 = \mathbf{P}_4 = \mathbf{0}$. The force \mathbf{P}_3 and \mathbf{P}_6 are calculated from:

$$\begin{bmatrix} P_3 \\ P_6 \end{bmatrix} = -\frac{EI_0}{L} \begin{bmatrix} m_{ii} & m_{ij} \\ m_{ji} & m_{jj} \end{bmatrix} \begin{bmatrix} q_i \\ q_j \end{bmatrix} \quad (28)$$

where θ_i and θ_j are the rotations at the ends of the member due to the span load $\mathbf{Q}(\mathbf{x})$. Using the conjugate beam method, these rotations, which are also given by Timoshenko and Young (1965), can be expressed as:

$$q_i = -\frac{1}{EL} \int_0^L \frac{\bar{M}(x)(L-x)}{I(x)} dx$$

$$q_j = \frac{1}{EL} \int_0^L \frac{\bar{M}(x)x}{I(x)} dx \quad (29)$$

where $\bar{M}(x)$ is the moment function due to span load $\mathbf{Q}(\mathbf{x})$ of the simply supported beam. The numerical integration is used for the calculations of θ_i and θ_j in eq. (29). Adding rotations for the different loads and substituting into eq. (28) yields the fixed end forces \mathbf{P}_3 and \mathbf{P}_6 . Then \mathbf{P}_2 and \mathbf{P}_5 can be calculated by adding the respective simply supported beam and end rotations and the reactions due to the end moments.

Deformations of the cross section due to transverse shear will produce additional deflection which is calculated by using the Bernoulli-Euler beam theory. The non-prismatic member shown in Fig.1 is subjected to member forces $\mathbf{Q}(\mathbf{x})$. Adding shear deformations over the length, the net deflection at end j with respect to origin i can be expressed as:

$$U_{5\ shear} = \frac{a}{G} \int_0^L \frac{\bar{V}_1(x) + V_2}{A(x)} dx \quad (30)$$

where $\bar{V}_1(x)$ is the function of shear force for the simply supported beam, which is obtained by differentiating the $\bar{M}(x)$ function with respect to x , and V_2 is the constant shear force due to end moments. From equilibrium,

$$V_2 = -\frac{EI_0}{L} [(m_{ii} + m_{ij})q_i + (m_{ij} + m_{jj})q_j] \quad (31)$$

Therefore, $U_{5\ shear}$ can be calculated by using numerical integration.

Additional fixed end forces caused by shear effects are the fixed end forces that will prevent $U_{5\ shear}$ in the beam. If the span load and the non-prismatic member are symmetric, then $U_{5\ shear} = 0$ and the additional fixed end forces will also equal to zero. Otherwise, a correction factor due to shear can be determined from eq. (1) and eq. (2) as follows:

$$\begin{bmatrix} P_2 \\ P_3 \\ P_5 \\ P_6 \end{bmatrix}_{shear} = b \frac{EI_0}{L^2} \begin{bmatrix} -(m_{ii} + m_{jj} + 2m_{ij}) \\ L \\ -(m_{ii} + m_{jj}) \\ (m_{ii} + m_{jj} + 2m_{ij}) \\ L \\ -(m_{ij} + m_{jj}) \end{bmatrix} U_{5\ shear} \quad (32)$$

Finally, the vector \mathbf{P} is determined by assigning the corresponding components of the fixed end forces due to axial forces, bending and shear.

Numerical Example

For the fixed ends haunched beam shown in Fig .6, the elastic modulus of concrete, E , is taken as 30 GPa, the shear modulus, G , as 12 GPa, the shape factor for shear, α , as 1.2 (for rectangular cross section), and member width is 0.4m.

The beam is analyzed by using the proposed method for mid-span heights, h , of 0.5, 0.75, 1.0, 1.25, and 1.5m. Fixed end moments at the left and right supports are determined with and without the transverse shear deformations. The results are compared with that obtained using the well-known finite element analysis program SAP90. For SAP90 analysis, the beam is divided into 48 subelements having constant area and moment of inertia defined at mid-section of each element with and without considering the effect of transverse shear deformations. The result of analysis is shown in Table

1A and Table 1B for both typed of analysis. When shear deformation is considered, the end moments increase. It is clear that the effect of shear deformations increases as the depth to span ratio increases.

Conclusions:

1-The derived stiffness matrix is general and applicable to simple bending theory, and cover a wide range of depth variation for haunched beams.

2-The proposed formulation is also general and can be used for other types of non-prismatic or haunched members.

3-Fixed end forces due to transverse shear deformations are considered, therefore more accurate results can be obtained in the case of high depth to span ratios.

4-Members with haunches can be analyzed as one element. This will reduce the number of equations, input data, time and effort compared to the analysis method of dividing into prismatic subelements, and that is very useful in frame analysis with non-prismatic members.

5-The proposed element is convenient to use with the general displacement method. It can be adapted to any finite elements analysis program.

List of Symbols :

a subdivision length (Fig. 5)

A, B left and right support reaction

A_i, A_j cross sectional area at *i* and *j* ends

A(x) ross section area of the beam

A₀ min. area of the member cross section

\bar{A}_0 min. area along the

length **\bar{L}**

C matrix of the coeff. in eq. (6)

E modulus of elasticity

F member force vector

F₁.. F₆ member forces

G shear modulus

I_i, I_j moment of inertia at *i* and *j* ends

I(x) moment of inertia at *x* from origin

I₀ min. moment of inertia of member cross section

I₁ ... I₄ integrals given in eqs.(5) and (12)

I₅ integral given in eq. (25b)

K₂₃, k₆₃ stiffness coeff. for $U_3=1$

\bar{K} , \bar{k}_{11} beam stiffness with neglecting axial deformation

K member stiffness matrix

L length of member

L_i, L_j length in variable left and right haunches

L₀ length in the constant mid-section.

\bar{L} subdivision length

M(x) moment function of the beam

$\bar{M}(x)$ moment function due to span load (x) of simply supported beam

n_{ii}, m_{ii}, m_{jj}, m_{ij} factors of the basic stiffness coefficients

\bar{n}_{ii} factor of the stiffness coeff. for length **\bar{L}**

P member fixed end

forces vector
 $\mathbf{P}_1.. \mathbf{P}_6$ fixed end forces
 $\mathbf{q}(\mathbf{x})$ addition of q_1 and q_2
 $\mathbf{q}_1, \mathbf{q}_2$ $M(\mathbf{x})/EI(\mathbf{x})$ function
 due to left right
 moment
 \mathbf{Q} load intensity
 $\mathbf{Q}(\mathbf{x})$ span load function
 \mathbf{U} member displacement
 vector
 $\mathbf{U}_1.. \mathbf{U}_6$ member disp.
 $\mathbf{U}_{2\text{shear}}$ shear deflection
 $\mathbf{U}_{5\text{shear}}$ total shear
 deflection of non-
 prismatic member at
 right end
 $\bar{\mathbf{V}}_1(\mathbf{x})$ function of shear
 force for simply
 supported beam
 \mathbf{V}_2 constant shear force due
 to end moment
 \mathbf{a} shape factor for shear
 $\mathbf{a}_i \mathbf{a}_j$ taper factor at the
 left and right
 haunches
 $\mathbf{b}, \mathbf{G}_1, \mathbf{G}_2, \mathbf{G}_3$ shear
 consideration factors
 $\Delta \mathbf{L}$ total axial elongation in
 length \mathbf{L}
 δ_Q disp. of point i due to
 the actual force \mathbf{Q}
 δ_{P1} disp. of point i due to $\mathbf{P1}$

 θ_i, θ_j rotations at the left
 and right supports of
 the simply support
 beam
 ψ factor defined in eq.
 (16)

References:

Al-Gahtani, H.J., 1996. Exact
 Stiffness Matrix for Tapered
 Members. ASCE Journal of

Structural Engineering, Vol. 122,
 No. 10: 1234-1239.

Al-Mezini, N. and Balkaya, C., 1991.
 Analysis of Frames with Non-
 Prismatic Members, ASCE Journal
 of Structural Engineering, Vol. 117,
 No. 6: 1537-1592.

Funk, R.R. and Wang, K., 1988
 .Stiffness of Non-Prismatic
 Members, ASCE Journal of
 Structural Engineering, Vol. 114,
 No. 2: 489-494

Popov, E.P., 1968. Introduction to
 Mechanics of Solids . Prentice- Hall,
 Inc., Englewood Cliffs , New York.

Reynolds, C.E. and Steedman, J.C
 , 1988. Reinforced Concrete
 Designer Handbook, 10th ed.,
 London, E. & F.N. SPON.

Timoshenko, S.P. and Young, D.H. ,
 1965. Theory of Structures.
 McGraw-Hill Book Co., Inc. , New
 York , N.Y.

Norris, C.H., Wilbur, J.B. and
 Utku, F., 1982. Elementary
 Structural Analysis. McGraw-Hill
 Book Co., Inc. , New York , N.Y.

Vanderbilt, M.D., 1978. Fixed End
 Action and Stiffness Matrices for
 Non-Prismatic Beams. Journal of
 American Concrete Institute. Vol.
 75, No. 7, pp. 290-298.

Appendix A :**Depth Equations for Haunches :****(1) Stepped Haunches :**

$$h(x)=h_i=\text{const.}$$

$$\text{for } 0 \leq x \leq L_i$$

$$h(x)=h_o=\text{const.}$$

$$\text{for } L_i \leq x \leq (L_i+L_o)$$

$$h(x)=h_o=\text{const.}$$

$$\text{for } (L_i+L_o) \leq x \leq L$$

(2) Linear Haunches:

$$h(x)=h_i-\alpha_i \cdot \text{for } 0 \leq x \leq L_i$$

$$h(x)=h_o=\text{const. for } L_i \leq x \leq (L_i+L_o)$$

$$h(x)=h_i-\alpha_i(L-x) \text{ for } (L_i+L_o) \leq x \leq L$$

(3) Parabolic Haunches :

$$h(x)=\alpha_i x^2 / L_i - 2\alpha_i x + h_i$$

$$\text{for } 0 \leq x \leq L_i$$

$$h(x)=h_o=\text{const. for } L_i \leq x \leq (L_i+L_o)$$

$$h(x)=\alpha_i (x^2 - 2(L-L_i)x + (L-L_i)^2) / L_i + h_o$$

$$h_o$$

$$\text{for } (L_i+L_o) \leq x \leq L$$

**Table 1A: Fixed end moments,
kN.m
(Proposed Analysis)**

	h,m	0.5	0.7 5	1.0	1.2 5	1.5
Left support	With Shear effect	29 5.3	276 .7	263 .9	254 .6	247 .7
	W/O shear effect	29 0.7	269 .1	253 .3	241 .0	231 .0
Right support	With Shear effect	- 54. 7	- 62. 6	- 67. 1	- 69. 9	- 71. 7
	W/O shear effect	- 58. 8	- 69. 4	- 76. 7	- 82. 3	- 87. 0

**Table 1B: Fixed end moments,
kN.m
(Finite Element Analysis Using
SAP90)**

	h,m	0.5	0.75	1.0	1.25	1.5
Left support	With Shear effect	295. 23	276. 91	263. 94	254. 51	247. 94
	W/O shear effect	290. 44	269. 25	253. 40	240. 90	231. 13
Right support	With Shear effect	- 54.8 7	- 62.6 3	- 67.1 7	- 69.9 5	- 71.6 4
	W/O shear effect	- 58.9 2	- 69.4 5	- 76.6 6	- 82.3 3	- 86.8 6

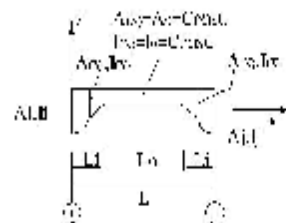


Fig.1: Haunched member with variable area and moment of inertia

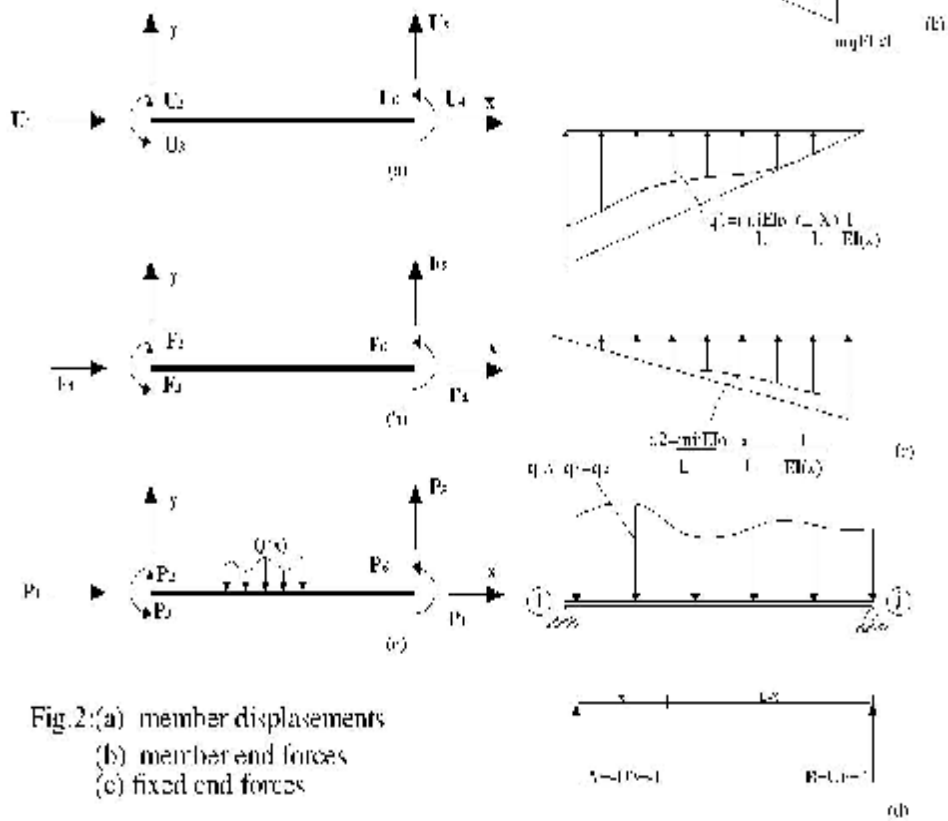


Fig.2:(a) member displacements
(b) member end forces
(c) fixed end forces

Fig.3: The $U_1=1$ loading and conjugate beam system :

- (a) $U_1=1$ loading
- (b) moment diagram for real beam
- (c) M/EI diagram of real beam
- (d) conjugate beam

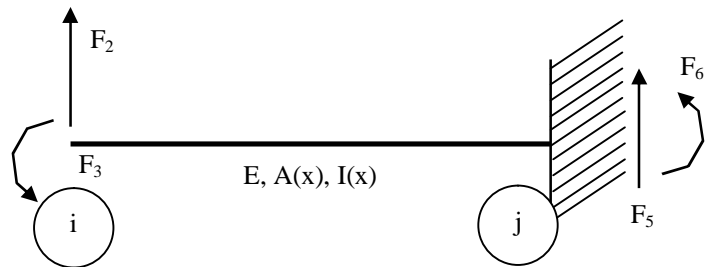


Fig.4: Non-prismatic member
Subjected to F_2 and F_3

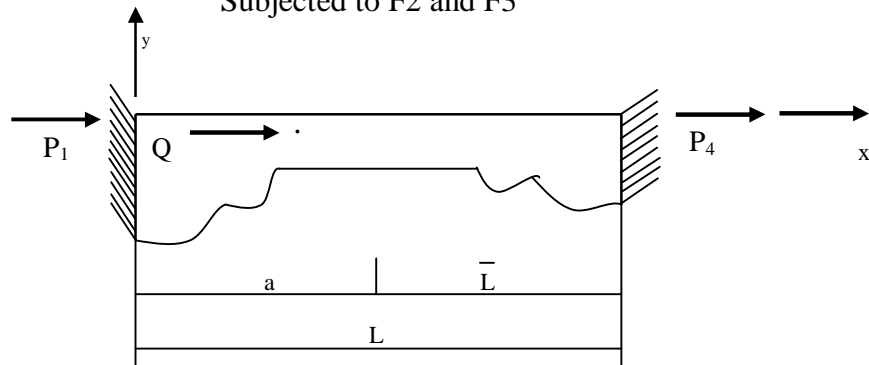


Fig.5: Axially loaded member

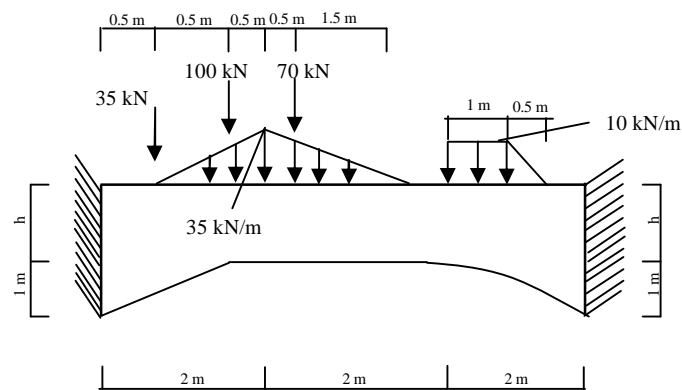


Fig.6: Numerical example